Journal of Applied Mathematics and Physics, 2022, 10, 1898-1909
https://www.scirp.org/journal/jamp
ISSN Online: 2327-4379
ISSN Print: 2327-4352

Relationship between Solar Activity, Total Ozone, and Solar Ultraviolet Radiation: Multifractal Analysis

Fumio Maruyama

Department of Sports and Health Science, Matsumoto University, Matsumoto, Japan
Email: fmaruya@nagoya-u.jp

How to cite this paper: Maruyama, F. (2022) Relationship between Solar Activity, Total Ozone, and Solar Ultraviolet Radiation: Multifractal Analysis. *Journal of Applied Mathematics and Physics*, **10**, 1898-1909.
https://doi.org/10.4236/jamp.2022.106130

Received: May 23, 2022
Accepted: June 21, 2022
Published: June 24, 2022

Abstract

We investigated the relationship between solar activity, total ozone, and solar ultraviolet B (UV-B) radiation from the perspective of multi-fractality. Fractal properties are observed in the time series of the dynamics of complex systems. To detect the changes in fractality, we performed a multifractal analysis using a wavelet transform. The changes in fractality indicated that solar activity was closely related to the total ozone and that the total ozone had a strong effect on UV-B radiation. For high solar activity, the F10.7 flux and global total ozone exhibited monofractality. The F10.7 flux and total ozone also increased, and a change from multifractality to monofractality was observed. This corresponded to the formation of the order. The strong interactions between the solar flux and ozone occur during the high solar activity. In contrast, UV-B radiation increased and showed multifractality, when fluctuations in UV-B radiation became large. For low solar activity, the F10.7 flux and total ozone exhibited multifractality, and UV-B radiation exhibited monofractality. Hence, the change in fractality of the F10.7 flux and total ozone was the opposite of UV-B radiation. A significant change in fractality for F10.7 flux and SSN, which had a significant fluctuation and a slight change in fractality for UV-B radiation, and total ozone were identified.

Keywords

Solar Flux, Total Ozone, UV-B Radiation, Wavelet, Multifractal

1. Introduction

In the early 1970s, Molina and Rowland proposed that chlorofluorocarbons, widely used as refrigerants and propellants, would reach the stratosphere and

catalyze the destruction of ozone molecules [1]. In 1985, evidence of an ozone hole over Antarctica was first published [2], and its progression over the ensuing years has been captured in images that have become symbols of human influence on the global environment.

There are significant effects of changes in the intensity of solar UV-radiation resulting from stratospheric ozone depletion, particularly UV-B radiation, on all organisms on the planet [3]. If there is a decrease of 1% in the slant ozone value, then the UV-B values increase by 1.0014% and 1.05% for the daily and monthly mean values in cloudless sky conditions, respectively [4]. Williamson *et al.* [5] highlighted the complex interactions between the drivers of climate change and those of stratospheric ozone depletion, and the positive and negative feedbacks among climate, ozone, and ultraviolet radiation. Bornman *et al.* [6] have broadened our understanding of the linkages that exist between the effects of ozone depletion, UV-B radiation, and climate change on terrestrial ecosystems.

Various objects in nature exhibit self-similarity or fractal properties. Monofractal shows an approximately similar pattern at different scales and is characterized by a fractal dimension. Multifractal is a non-uniform, more complex fractal and is decomposed into many sub-sets characterized by different fractal dimensions. Fractal properties can also be observed in time series representing the dynamics of complex systems. A change in fractality accompanies a phase transition and changes in the state. The multifractal properties of daily rainfall were investigated in two contrasting climates: an East Asian monsoon climate with extreme rainfall variability and a temperate climate with moderate rainfall variability [7]. In both climates, the frontal rainfall shows monofractality and the convective-type rainfall shows multifractality.

Hence, climate change can be interpreted from the perspective of fractals. A change in fractality may be observed when the climate changes. We attempt to explain climate changes, referred to as regime shifts, by analyzing their fractality. We used a wavelet transform to analyze the multifractal behavior of the climate index. Wavelet methods are useful for analyzing complex non-stationary time series. The wavelet transform allows reliable multifractal analysis to be performed [8]. In our previous paper [9], in terms of multifractal analysis, we concluded that a climatic regime shift corresponds to a change from multifractality to monofractality of the Pacific Decadal Oscillation index.

This study investigated the relationship between solar activity, total ozone, and UV-B radiation from the viewpoint of multi-fractality. To detect the changes in fractality, we examined multifractal analysis using a wavelet transform. It also aims to know in detail UV-B radiation that affects human health.

2. Data and Method of Analysis

The solar radio flux at 10.7 cm (F10.7 flux) provided by NOAA's space weather prediction center (http://www.swpc.noaa.gov/) was used. The F10.7 flux is an excellent indicator of the solar activity. We used the monthly sunspot number (SSN) provided by the Solar Influences Data Analysis Center (sidc.oma.be) and

the solar polar field throughout the solar sunspot cycle provided by the Wilcox Solar Observatory (wso.stanford.edu). The amount of UV-B radiation is the value obtained by integrating UV intensity from 280 to 315 nm in the wavelength range, and we used the observations in Tsukuba, Japan by the Japan Meteorological Agency. We used the global average total ozone provided by NASA (nasasearch.nasa.gov), obtained from satellite observations. We also used the total ozone in Tsukuba provided by the Japan Meteorological Agency. Total ozone is defined as the amount of ozone contained in a vertical column with a base area of 1 cm^2 at standard pressure and temperature.

We used the Daubechies wavelet as the analyzing wavelet because it is widely used in solving a broad range of problems, for example, self-similarity properties of a signal or fractal problems and signal discontinuities. The data used were a discrete signal that fitted the Daubechies Mother wavelet, with the capability of precise inverse transformation. Hence, the precise optimal value of $\tau(q)$ can be calculated as follows. We then estimated the scaling of the partition function $Z_q(a)$, which is defined as the sum of the q-th powers of the modulus of the wavelet transform coefficients at scale a. In our study, the wavelet-transform coefficients did not become zero, and therefore, for a precise calculation, the summation was considered for the entire set. Muzy *et al.* [8] defined $Z_q(a)$ as the sum of the q-th powers of the local maxima of the modulus to avoid division by zero. We obtained the partition function $Z_q(a)$:

$$Z_q(a) = \sum \left| W_\varphi [f](a,b) \right|^q , \tag{1}$$

where $W_\varphi[f](a, b)$ is the wavelet coefficient of the function f, a is a scale parameter and b is a space parameter. The time window was set to 6 years for the following reasons. We calculated the wavelets using a time window of 10, 6, and 4 years. For a time window of 10 years, a slow change in fractality was observed. Thus, this case was inappropriate for finding a rapid change because when we integrated the wavelet coefficient over a wide range, small changes were canceled. For 4 years, a rapid change in fractality was observed. The overlap of the first and subsequent data was 3 years, which is shorter than the 9 years in the case of the 10-year calculation and thus the change in fractality was large. For 6 years, a moderate change in fractality was observed and hence the time window was set to this period. For small scales, we expect

$$Z_q(a) \sim a^{\tau(q)} . \tag{2}$$

First, we investigated the changes in $Z_q(a)$ in a time series at a different scale a for each q. A plot of the logarithm of $Z_q(a)$ against the logarithm of the time scale a was created. Here $\tau(q)$ is the slope of the linear fitted line on the log-log plot for each q. Next, we plot $\tau(q)$ vs. q. The time window was then shifted forward for one year, and the process was repeated. We define monofractal and multifractal as follows: if $\tau(q)$ is linear with respect to q, then the time series is said to be monofractal: if $\tau(q)$ is convex upward with respect to q, then the time series is classified as multifractal [10]. We define the value of R^2, which is the

coefficient of determination, for the fitting straight line, if $R^2 \geq 0.98$ the time series is monofractal and if $0.98 > R^2$, which is multifractal.

We calculated the multifractal spectrum $\tau(q)$ of the SSN from 1910 to 2010, and that from 1967 to 1979 is shown in Figure 1. The data were analyzed in six-year sets; for example, the multifractal spectrum $\tau(q)$ of s67 was calculated between 1967 and 1972. To study the change in fractality, the time window was advanced by one year, and the multifractal spectrum $\tau(q)$ was obtained from s67 to s76. A monofractal signal corresponds to a straight line for $\tau(q)$, whereas for a multifractal signal, $\tau(q)$ is nonlinear. In Figure 1, the constantly changing curvature of the $\tau(q)$ curves for s67, s68, s72, s73, and s74 suggest multifractality. In contrast, $\tau(q)$ is linear for s69 - s71, indicating monofractality.

We plotted the value of $\tau(-6)$ for each index. The large negative value of $\tau(-6)$ indicates large multifractality. For $\tau(q)$, $q = -6$ is the appropriate number to show the change in τ.

3. Results

3.1. Relationship between the F10.7 Flux and UV-B Radiation

The solar radio flux at 10.7 cm (F10.7 flux) is shown in Figure 2(a). The amount of UV-B radiation obtained by integrating the UV intensity from 280 to 315 nm in the wavelength range in Tsukuba, Japan is shown in Figure 2(b). The maximum values changed, but the minimum values remained almost constant. UV-B radiation changed seasonally and reached a minimum during winter. The $\tau(-6)$ of the F10.7 flux and UV-B radiation are shown in Figure 3. A complicated graph can be converted into a simple graph from a fractal viewpoint. The red square shows monofractality and the green circle shows multifractality for the 6 years centered on the year plotted. For example, the green circle for 2000 in the F10.7 flux shows multifractality between 1997 and 2002. The data were excluded from Figure 3 for cases where we could not distinguish between monofractality and multifractality.

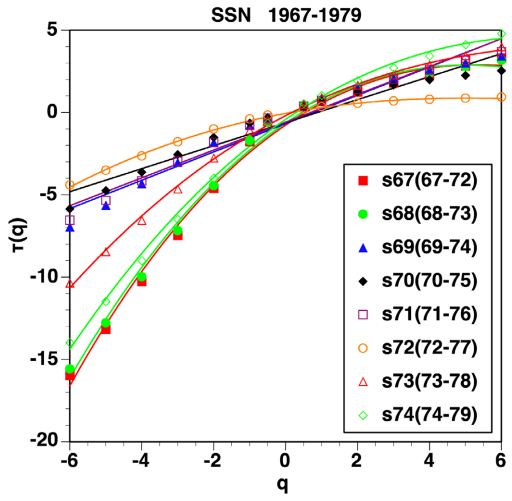

Figure 1. $\tau(q)$ for individual SSN between 1967 and 1979.

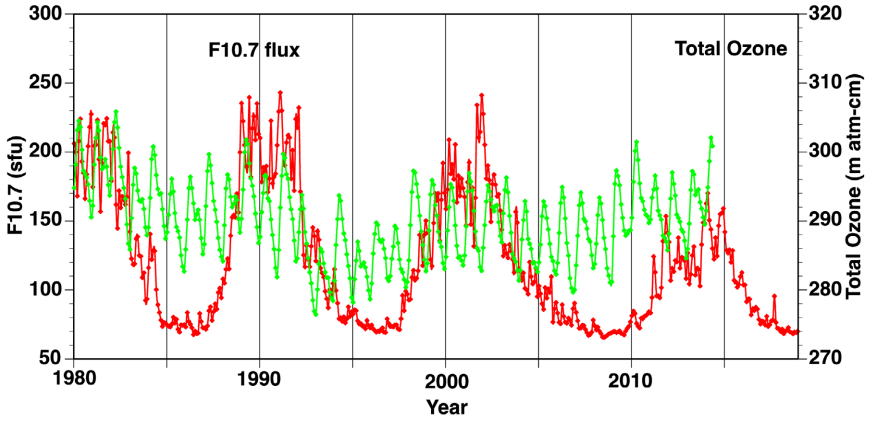

(a)

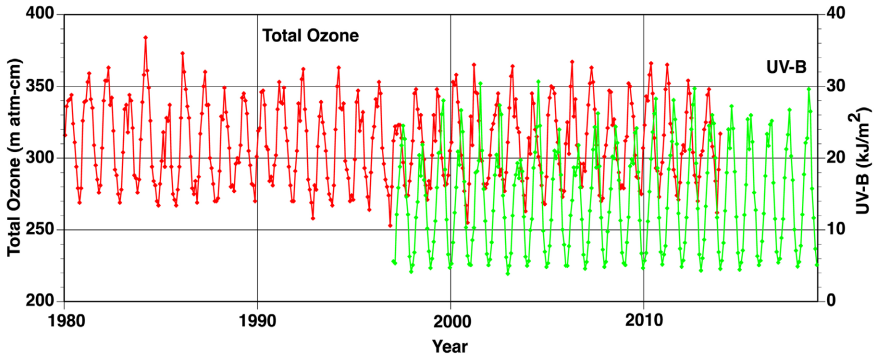

(b)

Figure 2. (a) F10.7 flux and global average total ozone; (b) The amount of UV-B radiation obtained by integrating the UV intensity from 280 to 315 nm in the wavelength range and total ozone in Tsukuba, Japan.

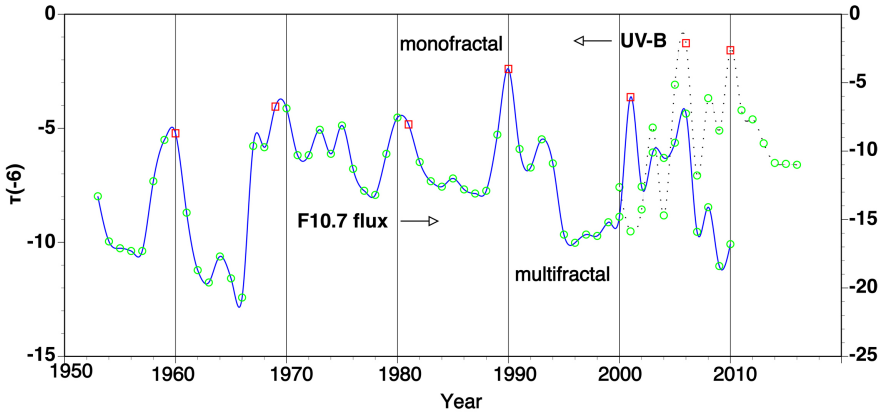

Figure 3. The $\tau(-6)$ of F10.7 flux, and UV-B radiation.

When the SSN was maximum, and the solar activity was high, the F10.7 flux became monofractal, and UV-B radiation became multifractal in 2001. When the SSN was minimum, and the solar activity was low, the F10.7 flux became multifractal, and UV-B radiation became monofractal in 2006 and 2010. But other than that, for the F10.7 flux and UV-B radiation, changes in fractality were

similar. Both show that they have the same radiation from the sun.

The $\tau(-6)$ density plots of F10.7 flux and UV-B radiation are shown in Figure 4(a) and Figure 8(a), respectively. For UV-B radiation, the density distribution had a single peak, and the distribution was narrow, showing small fractality changes. In contrast, for the F10.7 flux, the density distribution had two peaks and the distribution was wide, and the multifractality was strong.

3.2. Relationship between the SSN and UV-B Radiation

The $\tau(-6)$ of SSN and UV-B radiation are shown in Figure 5. When the SSN was minimum in 2010, the SSN became multifractal and UV-B radiation became monofractal. But other than that, for the SSN and UV-B radiation, the changes in fractality were similar, which showed that SSN was related to radiation intensity.

The $\tau(-6)$ density plot of the SSN is shown in Figure 4(b). The density distribution had two peaks and the distribution was wide and the multifractality was strong.

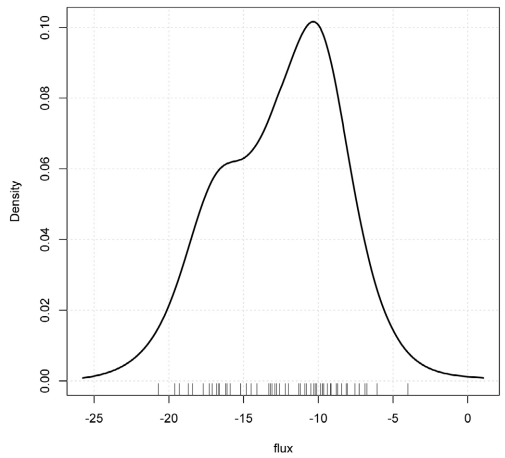

(a)

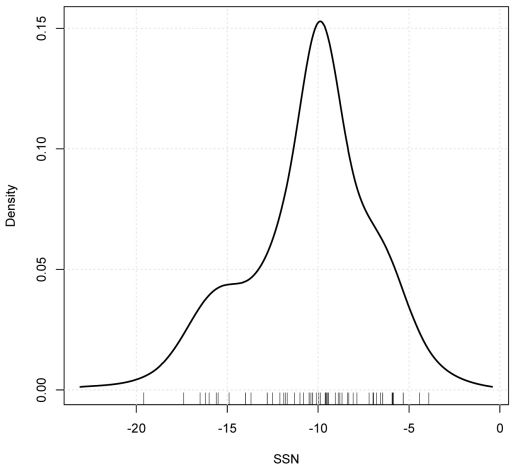

(b)

Figure 4. The $\tau(-6)$ density plots of F10.7 flux (a) and SSN (b).

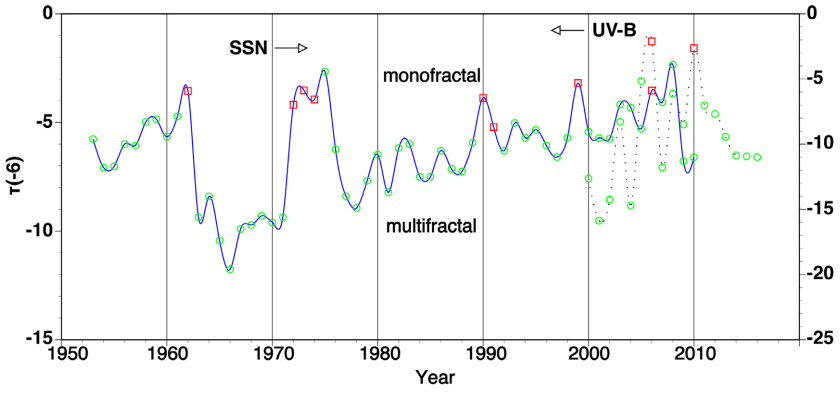

Figure 5. The $\tau(-6)$ of SSN, and UV-B radiation.

3.3. Relationship between the F10.7 Flux and Global Total Ozone

Figure 2(a) shows the F10.7 flux and global average total ozone. For high solar activity in 1990, the total ozone increased, and for low solar activity in 1996, which decreased. The global average total ozone decreased for low solar activity. For 1993-1998, the total ozone decreased.

The $\tau(-6)$ of the F10.7 flux, and total ozone are shown in Figure 6(a). For high solar activity during 1988-1990 and 2001-2002 as shown in Figure 2(a), monofractality was observed in both. In contrast, for low solar activity during 1996-1998, and 2007-2010, multifractality was strong in both. The correlation coefficient between F10.7 flux and total ozone was r = 0.35, and there was a weak positive correlation.

The lead of $\tau(-6)$ for the F10.7 flux was observed. The F10.7 flux significantly led to total ozone from the cross-correlation functions (CCF). In the total ozone, and F10.7 flux, the similar changes were observed, and those were related based on changes in fractality.

We show the wavelet coherence and phase using the Morlet wavelet between the total ozone and F10.7 flux in Figure 6(b). The coherence between the total ozone and F10.7 flux was strong, especially around 1990, and the lead in the F10.7 flux was observed.

3.4. Relationship between the Total Ozone and UV-B Radiation

In Tsukuba, Japan, the total ozone and UV-B radiation are shown in Figure 2(b). Seasonal changes were observed in both. The total ozone was the highest in spring and lowest in autumn. This is because large-scale transport of the stratospheric atmosphere from the equatorial region to mid-high latitudes is most active from winter to spring. UV-B radiation was the highest in summer and lowest in winter. The lead in the total ozone was observed. In 2003 the total ozone increased, and in 2004 the maximum of UV-B radiation became small. When the total ozone reached maximum, UV-B radiation was small because it was largely absorbed.

The $\tau(-6)$ of the total ozone, and UV-B radiation are shown in Figure 7(a). For high solar activity in 2002, the multifractality of the total ozone became weak

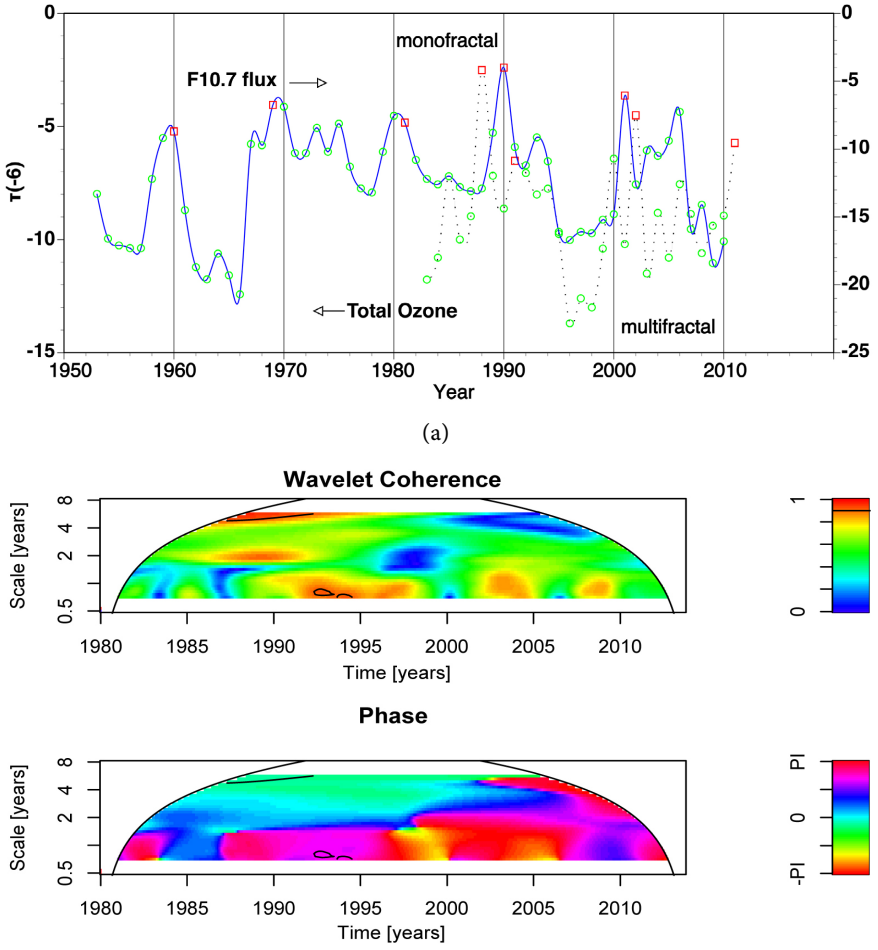

Figure 6. The $\tau(-6)$ of F10.7 flux, and global average total ozone (a). Wavelet coherence and phase between F10.7 flux and total ozone (b). The thick black contour encloses regions of greater than 95% confidence. The thin black contour encloses regions of greater than 90% confidence. The cone of influence, which indicates the region affected by edge effects, is shown with a black line. In the wavelet phase, the positive value shown by the blue and pink shading means that F10.7 flux leads total ozone and the negative value shown by the green, yellow and red shading means that total ozone leads F10.7 flux.

and multifractality became strong for UV-B radiation, when the total ozone increased, and UV-B radiation increased. For low solar activity between 2006 and 2010, multifractality of the total ozone became strong and monofractality was observed for UV-B radiation, when the total ozone decreased and UV-B radiation decreased because of the decrease in F10.7 flux. The lead in the total ozone was observed. The correlation coefficient between total ozone and UV-B was r = −0.28, and there was a weak negative correlation.

We show the wavelet coherence and phase using the Morlet wavelet between the total ozone in Tsukuba and UV-B radiation in Figure 7(b). The coherence between the total ozone and UV-B radiation was strong, and a half-year lead for the total ozone was observed. The strong influence of ozone on UV-B radiation was shown based on changes in fractality.

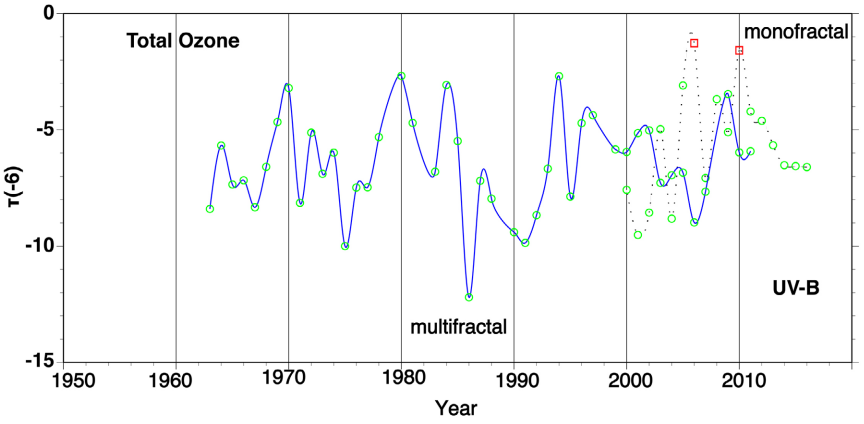

(a)

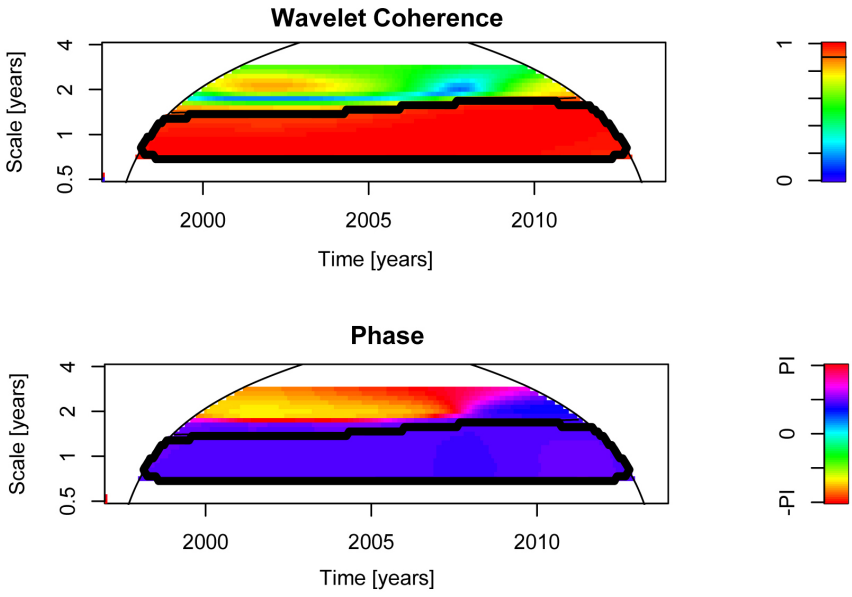

(b)

Figure 7. As for **Figure 6** but for the total ozone, and UV-B radiation in Tsukuba, Japan. In the wavelet phase, the positive value shown by the blue and pink shading means that total ozone leads UV-B radiation and the negative value shown by the green, yellow and red shading means that UV-B radiation leads total ozone.

The $\tau(-6)$ density plots of global total ozone and UV-B radiation are shown in **Figure 8(a)** and **Figure 8(b)**, respectively. Both the density distributions had a single peak, and the distribution was narrow, indicating a slight change in fractality.

4. Discussion

For high solar activity during 1988-1990 and 2001-2002, the F10.7 flux and total ozone exhibited monofractality, and UV-B radiation exhibited multifractality. The F10.7 flux and total ozone also increased as shown in **Figure 2(a)**, and a change from multifractality to monofractality was observed and those states became stable, which corresponded to the formation of order. In contrast, UV-B

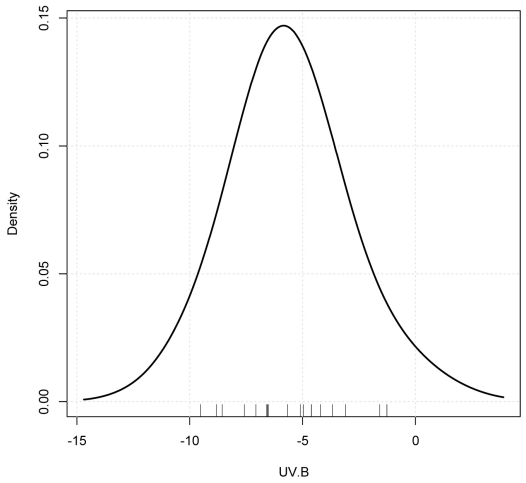

(a)

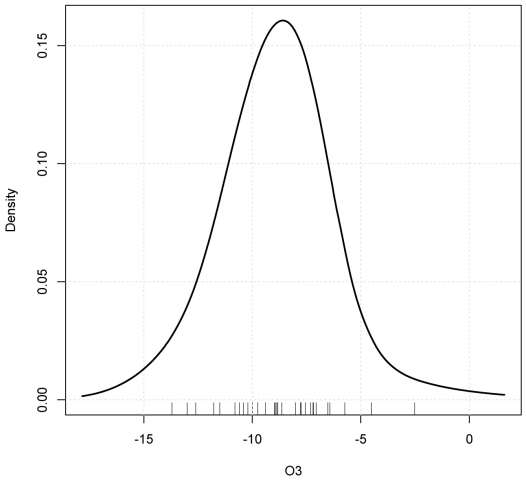

(b)

Figure 8. The $\tau(-6)$ density plots of UV-B radiation (a) and global average total ozone (b).

radiation decreased and showed multifractality, when fluctuations in UV-B radiation became large.

In a coupled chaos model, coupled chaos is a system composed of chaos which interacts with each other, an anomalous enhancement of the magnitude of the fluctuation is observed at the phase synchronization point [11]. In other words, an increase in fluctuation is observed in a coupled chaos system just before chaos synchronization, which occurs when fractality and state change. Coupled chaotic systems have attracted the attention of many researchers as a good model that can realize the complicated phenomena of the natural world, and their dynamics can yield a wide variety of complex and strange phenomena [12]. For high solar activity, a mechanism similar to the coupled chaos system might exist, that is, coherence becomes strong, and fluctuations increase, and the multifractal behavior becomes strong, and a change from multifractal to monofractal behavior is observed. This implies that strong interactions between the solar flux and total

ozone occur for high solar activity. Strong interactions were inferred from the similarity of fractality changes and wavelet coherence. In particular, for 1988-1990 wavelet coherence was strong. The influence of solar activity on ozone was shown.

For low solar activity, the F10.7 flux, total ozone, and UV-B radiation decreased. The F10.7 flux and total ozone showed multifractality when fluctuations of F10.7 flux and total ozone became large. In contrast, UV-B radiation showed monofractality. Hence, the change in fractality of F10.7 flux and total ozone was the opposite of UV-B radiation.

The density distribution of the F10.7 flux and SSN had two peaks, and the distribution was wide, and the multifractality was strong. The global total ozone and UV-B had a single peak, and the distribution was narrow, indicating a slight change in fractality. We identified a significant change in fractality for F10.7 flux, and SSN, which had a significant fluctuation and a slight change in fractality for UV-B radiation, and total ozone.

5. Conclusions

We investigated the relationship between solar activity, total ozone, and UV-B radiation from the viewpoint of multifractality. To detect changes in fractality, we performed multifractal analysis using a wavelet transform. We showed changes in fractality by plotting the τ-function and used wavelet coherence. The main findings are summarized as follows:

1) The solar activity was closely related to the total ozone, and ozone had a strong effect on UV-B radiation based on changes in fractality.

2) For high solar activity, the F10.7 flux and global total ozone exhibited monofractality. The F10.7 flux and total ozone also increased, and a change from multifractality to monofractality was observed. This corresponded to the formation of the order. Strong interactions between the solar flux and ozone occur during the high solar activity. In contrast, UV-B radiation increased and showed multifractality, when fluctuations in UV-B radiation became large.

3) For low solar activity, the F10.7 flux and global total ozone exhibited multifractality, and UV-B radiation exhibited monofractality. Hence, the change in fractality of the F10.7 flux and total ozone was the opposite of UV-B radiation.

4) A significant change in fractality for F10.7 flux, and SSN, which had a significant fluctuation, and a slight change in fractality for UV-B radiation, and total ozone were identified.

Conflicts of Interest

The author declares no conflicts of interest regarding the publication of this paper.

References

[1] Molina, M. and Rowland, F. (1974) Stratospherec Sink for chlorofluoromethanes:

Chlorine Atomic-Catalysed Destruction of Ozone. *Nature*, **249**, 810-812. https://doi.org/10.1038/249810a0

[2] Farman, J.C., Cardiner, B.G. and Shanklin, J.D. (1985) Large Loss of Total Ozone in Antarctica Reveal Seasonal CLOx/NOx Interaction. *Nature*, **315**, 207-210. https://doi.org/10.1038/315207a0

[3] Solomon, K.R. (2008) Effects of Ozone Depletion and UV-B Radiation on humans and the Environment. *Atmosphere-Ocean*, **46**, 185-202. https://doi.org/10.3137/ao.460109

[4] Adam, M.E.N. (2010) Effect of Stratospheric Ozone in UVB Solar Radiation Reaching the Earth's Surface at Qena, Egypt. *Atmospheric Pollution Research*, **1**, 155-160. https://doi.org/10.5094/APR.2010.020

[5] Williamson, C.E., Zepp, R.G., Lucas, R.M., Madronich, S., Austin, A.T., Ballare, C. L., Norval, M., Sulzberger, B., Bais, A.F., Mckenzie, R.L., Robinson, S.A., Hader, D. P., Paul, N.D. and Bornman, J.F. (2014) Solar Ultraviolet Radiation in a Changing Climate. *Nature Climate Change*, **4**, 1-8. https://doi.org/10.1038/nclimate2225

[6] Bornman, J.F., Barnes, P.W., Robinson, A.A., Ballare, C.L., Flint, S.D. and Caldwell, M.M. (2015) Solar Ultraviolet Radiateon and Ozone Depleteon-Driven Climate Change: Effects on Terrestriall Ecosystems. *Photochemical and Photobiological Sciences*, **14**, 88-107. https://doi.org/10.1039/C4PP90034K

[7] Svensson, C., Olsson, J. and Berndtsson, R. (1996) Multifractal Properties of Daily Rainfall in Two Different Climates. *Water Resources Research*, **32**, 2463-2472. https://doi.org/10.1029/96WR01099

[8] Muzy, J.F., Bacry, E. and Arneodo, A. (1991) Wavelets and Multifractal Formalism for Singular Signals: Application to Turbulence Data. *Physical Review Letters*, **67**, 3515-3518. https://doi.org/10.1103/PhysRevLett.67.3515

[9] Maruyama, F., Kai, K. and Morimoto, H. (2015) Wavelet-Based Multifractal Analysis on Climatic Regime Shifts. *Journal of the Meteorological Society of Japan*, **93**, 331-341. https://doi.org/10.2151/jmsj.2015-018

[10] Frish, U. and Parisi, G. (1985) On the Singularity Structure of Fully Developed Turbulence, in Turbulence and Predictability in Geophysical Fluid Dynamics and Climate Dynamics. edited by Ghil, M., Benzi, R. and Parisi, G., North-Holland, New York, 84-88.

[11] Fujisaka, H., Uchiyama, S. and Horita, T. (2005) Mapping Model of Chaotic Phase Synchronization. *Progress of Theoretical Physics*, **114**, 289-299. https://doi.org/10.1143/PTP.114.289

[12] Wada, M., Kitatsuji, K. and Nishio, Y. (2005) Spatio-Temporal Phase Patterns in Coupled Chaotic Maps with Parameter Deviations. *Proceedings of* 2005 *International Symposium on Nonlinear Theory and Its Applications*, Bruges, 18-21 October 2005, 178-181.